HHS Public Access

Author manuscript

Science. Author manuscript; available in PMC 2015 December 12.

Published in final edited form as:

Science. 2015 June 12; 348(6240): aaa2340. doi:10.1126/science.aaa2340.

Inhibition of the Prostaglandin Degrading Enzyme 15-PGDH Potentiates Tissue Regeneration *

Yongyou Zhang[1,†], **Amar Desai**[1,†], **Sung Yeun Yang**[1,14,†], **Ki Beom Bae**[1,15,†], **Monika I. Antczak**[2,†], **Stephen P. Fink**[1,†], **Shruti Tiwari**[1,10,†], **Joseph E. Willis**[3,4,10], **Noelle S. Williams**[2], **Dawn M. Dawson**[3,4], **David Wald**[3,4,10], **Wei-Dong Chen**[1,++], **Zhenghe Wang**[3,5], **Lakshmi Kasturi**[1], **Gretchen A. Larusch**[1], **Lucy He**[1,‡‡], **Fabio Cominelli**[1,10], **Luca Di Martino**[1], **Zora Djuric**[6], **Ginger L. Milne**[11], **Mark Chance**[7], **Juan Sanabria**[8,10], **Chris Dealwis**[9], **Debra Mikkola**[1], **Jacinth Naidoo**[2], **Shuguang Wei**[2], **Hsin-Hsiung Tai**[12,¶], **Stanton L. Gerson**[1,3,10,*,¶], **Joseph M. Ready**[2,13,*,¶], **Bruce Posner**[2,13,*,¶], **James K. V. Willson**[13,*,¶], and **Sanford D. Markowitz**[1,3,10,*,¶]

[1]Department of Medicine, Case Western Reserve University, Cleveland, OH 44106, USA

[2]Department of Biochemistry, University of Texas Southwestern Medical Center, Dallas, TX 75390, USA

[3]Case Comprehensive Cancer Center, Case Western Reserve University, Cleveland, OH 44106, USA

[4]Department of Pathology, Case Western Reserve University, Cleveland, OH 44106, USA

[5]Department of Genetics and Genome Sciences, Case Western Reserve University, Cleveland, OH 44106, USA

[6]Department of Family Medicine, University of Michigan, Ann Arbor MI 48109, USA

[7]Proteomics Center, Case Western Reserve University, Cleveland, OH 44106, USA

[8]Department of Surgery, Case Western Reserve University, Cleveland, OH 44106, USA

[9]Department of Pharmacology, Case Western Reserve University, Cleveland, OH 44106, USA

[10]Case Medical Center, Cleveland, OH 44106, USA

[11]Department of Pharmacology, Vanderbilt University, Nashville, TN 37232, USA

*Correspondence to: SXM10@cwru.edu (SDM); James.Willson@UTSouthwestern.edu (JKVW); SLG5@cwru.edu (SLG); Joseph.Ready@utsouthwestern.edu (J MR); Bruce.Posner@UTSouthwestern.edu.

†These authors contributed equally to this work.

¶These authors contributed equally to this work.

++Present name and address: (Wei-Dong) David Chen, Genetics Branch, National Cancer Institute, National Institutes of Health, Bethesda, MD20892, USA

‡‡Present address: Department of Neurological Surgery, Vanderbilt University Medical Center, Nashville, TN 37232, USA

Supplementary Materials:
Materials and Methods
Figures S1-S20
Table S1
References (42–46)

[12]College of Pharmacy, University of Kentucky, Lexington, KY 40536, USA

[13]Simmons Cancer Center, University of Texas Southwestern Medical Center, Dallas, TX 75390, USA

[14]Department of Gastroenterology, Haeundae Paik Hospital, Inje University, Busan 612896, South Korea

[15]Department of Surgery, Busan Paik Hospital, and Paik Institute of Clinical Research and Ocular Neovascular Research Center, Inje University, Busan, South Korea

Abstract

Tissue regeneration is a medical challenge faced in injury from disease and during medical treatments such as bone marrow transplantation. Prostaglandin PGE2, which supports expansion of several types of tissue stem cells, is a candidate therapeutic target for promoting tissue regeneration in vivo. Here we show that inhibition of 15-hydroxyprostaglandin dehydrogenase (15-PGDH), a prostaglandin-degrading enzyme, potentiates tissue regeneration in multiple organs in mice. In a chemical screen, we identify a small-molecule inhibitor of 15-PGDH (SW033291) that increases prostaglandin PGE2 levels in bone marrow and other tissues. SW033291 accelerates hematopoietic recovery in mice receiving a bone marrow transplant. SW033291 also promotes tissue regeneration in mouse models of colon and liver injury. Tissues from 15-PGDH knockout mice demonstrate similar increased regenerative capacity. These findings raise the possibility that inhibiting 15-PGDH could be a useful therapeutic strategy in several distinct clinical settings.

INTRODUCTION

Tissue regeneration is a therapeutic challenge during recovery from many injuries, diseases, and disease treatments. For example, hematopoietic stem cell transplantation (HSC transplantation), that includes bone marrow transplantation, is a potentially curative therapy used in treating many hematologic malignancies (1). However, following HSC transplantation, individuals are at high risk of potentially lethal infections while awaiting regeneration of peripheral blood neutrophils, and are also at risk of internal bleeding while awaiting regeneration of platelets (1). Experimental approaches have principally focused on strategies that use ex vivo treatments to expand the numbers or increase the efficacy of donor hematopoietic stem cells prior to transplantation (2–4). In a different disease, ulcerative colitis, tissue damage to the colon epithelium, in part from immune cells, causes both gastrointestinal bleeding and diarrhea (5). Current treatments of ulcerative colitis primarily involve immune suppression, without available agents for potentiating healing and regeneration of the damaged colonic epithelium (5). Finally, tissue regeneration is a therapeutic requirement in liver surgery for cancer, where survival requires individuals' regaining adequate organ function after undergoing partial hepatic resection (6–8).

Prostaglandin PGE2 is a candidate molecule for potentiating regeneration in multiple different tissues. PGE2 is produced by the enzyme activity of cyclooxygenase-1 or cyclooxygenase-2 (COX-1 and COX-2) followed sequentially by that of prostaglandin E synthase (9). PGE2 augments Wnt signaling (10, 11), a pathway that is involved in the

maintenance of several types of tissue stem cells, including hematopoietic and colon stem cells (11, 12). PGE2, and its more stable analog 16, 16-dimethyl-PGE2 (dmPGE2), expand hematopoietic stem cell numbers in mice and in zebrafish (11, 13, 14). Murine bone marrow cells and human cord blood stem cells that are treated ex vivo with dmPGE2 show enhanced engraftment when these cells are injected back into recipient mice (4, 14–17). dmPGE2 treatment of human cord blood stem cells prior to their administration in human HSC transplants is currently being tested in clinical trials (4). PGE2 similarly supports the expansion of human colon stem cells in cell culture (18). And, in a model of murine colitis, colon injury was exacerbated by a COX enzyme antagonist but was ameliorated by treatment withdmPGE2 (19).

We hypothesized that alternative potential strategies for increasing PGE2 mediated tissue repair in vivo could be either to increase the synthesis of PGE2 or to inhibit the normally rapid in vivo degradation of PGE2. 15-hydroxyprostaglandin dehydrogenase (15-PGDH), that acts in vivo as a negative regulator of prostaglandin levels and activity (20–22), provides a candidate target. 15-PGDH catalyzes the first step in the degradation of prostanoid family molecules, oxidizing the prostanoid 15-hydroxyl group to a ketone, and thereby abrogating binding to prostaglandin receptors (20). Here we explore whether pharmacological inhibition of 15-PGDH can potentiate tissue repairin several mouse models of injury and disease.

Results

Genetic Deletion or Pharmacologic Inhibition of 15-PGDH Increases Tissue PGE2 Levels

To confirm that 15-PGDH broadly regulates PGE2 in vivo, we compared PGE2 levels in 15-PGDH knockout (21) and wild-type mice, retesting lung (21) and colon (22), and newly interrogating bone marrow and liver. Although basal PGE2 levels varied 5-fold across these four tissues, the 15-PGDH knockout mice exhibited a consistent 2-fold increase in PGE2 levels (Fig 1A). We hypothesized that a chemical inhibitor of 15-PGDH would have similar effect, and further, would provide a tool to explore 15-PGDH as a therapeutic target for potentiating tissue regeneration.

As a first step in exploring the therapeutic potential of pharmacologically inhibiting 15-PGDH, we conducted a high-throughput screen to identify small-molecule modulators of 15-PGDH enzyme activity. We screened 230,000 synthetic compounds in the University of Texas Southwestern Medical Center Chemical Library using a cell-based assay designed to identify compounds that might bind to and/or alter the stability or amount of 15-PGDH. Positive hits were then further tested to identify functional enzyme inhibitors. This approach identified the small molecule SW033291 (molecular weight: 412.59 Da) as a potent inhibitor of 15-PGDH enzyme activity (Fig. 1G). Initial characterization showed that treating cells with SW033291 decreased cellular 15-PGDH enzyme activity by 85% (Fig. S1A). In vitro incubations of this compound with recombinant 15-PGDH protein confirmed that SW033291 is a direct high-affinity inhibitor of 15-PGDH enzyme activity, with an inhibitor dissociation constant Ki^{app} =0.1 nM (23). As expected, the IC_{50} (concentration to inhibit 50% of enzyme activity in vitro) of SW033291 closely approximated 50% of any 15-PGDH concentration tested (e.g. IC_{50} of 1.5 nM SW033291 against 6 nM 15-PGDH) (Fig. S1, B-

D). SW033291 inhibition of 15-PGDH was non-competitive versus PGE2 over concentrations up to 40 μM PGE2 (Fig. S1E). SW033291 also demonstrated selective high affinity interaction with 15-PGDH in thermal denaturation assays. Specifically, SW033291 shifted the 15-PGDH melting temperature by 13.5°C (Fig. S2), but had no impact on the melting temperature of two other closely related short-chain dehydrogenases (S3). Treatment of A549 cells with SW033291 increased PGE2 levels by 3.5-fold at 500 nM, with 50% of maximal stimulation (EC50) at approximately 75 nM (Fig. S4).

Importantly, mice injected with SW033291 closely phenocopied 15-PGDH knockout mice, with 10 mg/kg SW033291 inducing a 2-fold increase in PGE2 levels in bone marrow, colon, lung and liver (Fig. 1B, S5). Prostaglandins PGD2 and PGF2a are also candidate substrates of 15-PGDH. Basal PGD2 levels were lower than PGE2 levels in all four mouse tissues examined, and showed a lesser, though still significant, induction with SW033291 (Fig. S6A). PGF2a tissue levels, which were lower still, were mostly unaltered by SW033291 (Fig. S6B). We detected no toxicity from chemical inhibition of 15-PGDH in adult mice. Mice injected with SW033291 at 20 mg/kg daily for 7 days showed equivalent daily weights and activity as mice injected with vehicle-control, and showed no adverse changes in blood counts or serum chemistry.

15-PGDH Inhibition Promotes Hematopoietic Recovery after Bone Marrow Transplantation

The ability of PGE2 to promote hematopoiesis has been documented by two types of experiments: (i) ex vivo treatment of hematopoietic stem cells with dmPGE2 improves stem cell engraftment and consequent survival of mice, and (ii) administration of PGE2 or dmPGE2 to sub-lethally irradiated mice accelerates hematopoietic recovery and increases numbers of the short-term subtype of hematopoietic stem cells (11, 13–17, 24–27). Previous work also revealed that dmPGE2-treated cells have increased levels of cyclic AMP, increased expression of CXCR4 and survivin, decreased apoptosis, and increased homing to the bone marrow stem cell niche (11, 14–16, 24, 25, 27).

To evaluate whether 15-PGDH might regulate these responses, we examined 15-PGDH knockout mice and SW033291 treated wild-type mice. We observed a significant 43% increase in neutrophil counts in 15-PGDH knockout versus wild-type mice (Fig. 1C), and a significant 39% increase in bone marrow SKL (Sca-1^+ C-kit^+ Lin^-) cells (Fig. 1D), which are enriched for bone marrow stem cells. There were no significant differences in counts of other peripheral blood cells, in bone marrow cellularity, or in numbers of bone marrow SLAM (Sca -1^+C -kit^+ Lin^- $CD48^-$ $CD150^+$) cells (that are further enriched for bone marrow stem cells) (Figs. S7 and S8, AC). Mice injected with SW033291 for three consecutive days showed similar significant benefits, including a doubling of peripheral neutrophil counts (Fig. 1E, S9), a 65% increase in marrow SKL cells (Fig. 1F), and a 71% increase in marrow SLAM cells (Fig. S10, A–C).

In functional assays, bone marrow from 15-PGDH knock-out mice and from SW033291-treated mice both showed significant 55% increases in the numbers of hematopoietic colonies generated after plating into methylcellulose (Fig. 2, A–B). Erythroid (BFU-E) and myeloid (CFU-GM) type colonies were each significantly increased in testing marrow from both 15-PGDH knockout mice (Fig. S8, D and E) and SW033291 treated mice (Fig. S10, D

and E). Likewise, ex vivo treatment of harvested bone marrow cells with SW033291 induced a significant 50% increase in hematopoietic colony formation (Fig. 2C), indicating that the compound acts directly on these cells. SW033291 did not increase colony formation of bone marrow from 15-PGDH knockout mice, confirming that the compound acts by directly targeting15 -PGDH (Fig. 2C).

To determine the effects of SW033291 on gene expression, we sorted bone marrow from control and SW033291-treated mice into SKL marked and $CD45^-$ fractions. In $CD45^-$ cells, which are enriched for bone marrow stromal cells, SW033291 treatment induced a greater than 4-fold and significant increased expression of CXCL12 and SCF (Figs. 2, D and E, and S11A). These two cytokines in the hematopoietic niche play key roles in hematopoietic stem cell homing and maintenance (28). No changes were seen in expression of CXCR4 or survivin, and JAG1 expression was not detected in either treated or untreated fractions (Fig. S11A). In SKL cells, SW033291 had no significant effects on expression of CXCL12, SCF, CXCR4, survivin, or JAG1 (Fig. S11B). Induction of CXCL12 and SCF in $CD45^-$ cells was significantly blocked when SW033291 was co-administered to mice together with an antagonist of EP4 or EP2 type PGE2 receptors (Fig. 2, D and E). However, SW033291 fully induced CXCL12 and SCF when co-administered with antagonists of EP1 or EP3 receptors (Fig. S11, C and D). As expected for activation of EP2 and EP4 receptors, SW033291 also increased cyclic AMP levels in$CD45^-$ cells (Fig. S11E). We conclude that SW033291 increases PGE2 levels within bone marrow, and that PGE2 functions through the EP2 and EP4 receptors to induce CXCL12 and SCF.

Having observed SW033291 treatment increases cytokines from the hematopoietic niche, we next determined if SW033291 would affect the ability of the mouse bone marrow to attract and support new hematopoietic stem cells. Accordingly, SW033291 or vehicle-control were administered to mice receiving a bone marrow transplant, and their respective abilities to attract new donor marrow cells to the transplant recipient's bone marrow were compared. Transplant recipient mice treated with SW033291 showed a significant 2- to 3-fold increase in the number of donor cells that homed to the recipient's bone marrow (Figs. 2, F and G, and S12). This effect of SW033291 could be blocked by co-treating the transplant recipient mice with: an inhibitor of PGE2 generation, an inhibitor of PGE2 signaling, or an antagonist of CXCL12 (that is induced by PGE2). Thus, the increased homing of donor bone marrow cells was significantly blocked when transplant recipient mice were co-treated with SW033291 plus: the COX inhibitor indomethacin (Fig. S12), or the EP4 antagonist L-161,982 (Fig. 2F), or the CXCL12 antagonist Plerixafor (Fig. 2G). An EP2 antagonist produced a weaker, though still significant, block of SW033291 effect (Fig. 2F). The SW033291-induced homing of transplanted donor bone marrow cells is thus driven, at least in part, by the induction of CXCL12 expression in $CD45^-$ non-myeloid cells that are already resident in bone marrow of recipient mice. Together these results define a pathway in which 15-PGDH inhibition causes an increase in bone marrow PGE2, which in turn induces expression of bone marrow CXCL12 and SCF, cytokines that alter the bone marrow microenvironment to better support the homing of transplanted cells.

To investigate whether 15-PGDH inhibition promotes hematopoietic recovery after a bone marrow transplant, we studied lethally irradiated mice that had been infused with 200,000

strain-matched donor bone marrow cells. Under these conditions, the transplanted cells on their own are insufficient to reconstitute hematopoiesis. We further treated these transplanted mice twice daily with intraperitoneal (IP) injections of either SW033291 (5 mg/kg) or vehicle-control, starting immediately after irradiation and continuing for 21 days. The control mice all died between study days 6 to 14 (Fig. 3A). In contrast, all of the SW033291-treated mice survived for over 30 days (Fig. 3A).

To characterize the hematopoietic recovery induced by SW033291, we examined the compound's effect on mice that were transplanted with 500,000 bone marrow cells. Under these conditions 63% of vehicle-control-injected mice, and all of the SW033291-treated mice, survived for 30 days, and hence were available for examination. In this experiment, SW033291-treated mice showed significantly accelerated recovery of neutrophils, platelets and red blood cells (Fig. 3, B–D). On day 12 after transplant, SW033291-treated mice had recovered 535 neutrophils/μl versus 182 neutrophils/μl in controls (Fig. 3B), differences that would likely be meaningful in a clinical setting. On day 18-post transplant, SW033291-treated mice reached 1380 neutrophils/μl versus 646 neutrophils/μl in controls (Fig. 3B). SW033291 thus accelerated neutrophil recovery in mice by nearly 6 days. SW033291-treated mice also showed a significantly accelerated platelet recovery and a significantly less severe platelet nadir (Fig. 3C). For example, on post-transplant day 8, SW033291-treated mice had 77,000 platelets versus 39,500 platelets in controls (Fig. 3C). Again, these differences would likely be meaningful in a clinical setting. SW033291 treated mice also showed accelerated red cell recovery (Fig. 3D). For example, hemoglobin levels on post-transplant day 12 were 10.7 g/dL in SW033291-treated mice versus 8.0 g/dL in control mice (Fig. 3D). In humans, these differences would likely translate to lesser need for transfusion support. More rapid recovery of peripheral blood counts in SW033291-treated mice reflected an accelerated and more robust engraftment in the bone marrow, as evidenced by these mice having a 2.4-fold significant increase in SKL bone marrow cells on post-transplant day 18 (Fig. 3E). SW033291 effectiveness in accelerating recovery of neutrophils, platelets, and red cells after bone marrow transplant is consistent with this compound increasing generation of both myeloid and erythroid colonies in cell culture assays.

While systemic administration of PGE2 has been suggested to have potentially negative effects on myelopoiesis (29) and on long term hematopoietic stem cells (24), no such adverse effects were seen with SW033291. In particular, in a repeat experiment, 8 of 10 mice transplanted with 500,000 donor bone marrow cells and receiving SW033291 injections for 21 days were alive 7 months later. This was comparable to 7 of 10 mice that were alive after receiving a similar transplant plus injections with vehicle-control. In a second assay to test for any long-term adverse effects of SW033291 on bone marrow stem cells, we harvested bone marrow from transplant recipient mice and challenged its capacity to reconstitute hematopoiesis when re-transplanted into a new cohort of irradiated recipient mice. Marrow originating from mice treated with SW033291 during a first transplant could in this manner be serially harvested and re-passaged for three successive rounds of: harvest, re-transplantation, marrow regeneration, and then repeat challenge by re-harvest and re-transplantation (Table S1). In this assay, the marrow harvested from mice receiving SW033291 during original transplant also showed equal long term robustness to the marrow harvested from mice injected with vehicle-control during original transplant, each achieving

an 80% success rate in reconstituting hematopoiesis at the third round of serial marrow transfer (Table S1). We suggest that the beneficial activity of SW033291 reflects its optimization of the physiology of both dose and route of delivery of PGE2, i.e., that inhibiting 15-PGDH generates increased PGE2 at physiologic levels and directly at tissue sites, and avoids the extremes of concentration accompanying administration by exogenous routes.

15-PGDH Inhibition Protects Mice From Colitis

To determine whether inhibiting 15-PGDH would promote regeneration in other tissues in which 15-PGDH inhibition increases PGE2, we examined the effects of 15-PGDH blockade in colons of mice treated for 7 days with oral dextran sodium sulfate (DSS), an agent that induces colonic ulcerations similar to those found in human ulcerative colitis (30) (Fig. 4, A and B). Mice treated daily with SW033291 and 15-PGDH knockout mice both showed marked resistance to DSS-induced colitis when compared to wild-type mice receiving vehicle-control. With either chemical or genetic ablation of 15-PGDH, there were 70% fewer colon ulcers counted on colonoscopy (Fig. 4C, days 11 and 15) and 87% less total area of ulcerated colon mucosa as measured by histomorphometry (Fig. 4D). SW033291-treated and 15-PGDH knockout mice showed marked suppression of mucosal inflammation by colonoscopic grading (MEICS score) (31) (Fig. 4F) and by histological cryptitis score (32) (Fig. 4, E and G). SW033291-treated (Figs. S13A, S14A) and 15-PGDH knockout mice (Fig. S14A) also show marked suppression of colitis symptoms, with significantly less diarrhea and rectal bleeding, as assessed by disease activity index (DAI)) (32). SW033291-treated (Figs. S13B, S14B) and 15-PGDH knockout mice (Fig. S14B) also showed significantly less weight loss, with SW033291 protection increasing with increasing dose. SW033291-treated and 15-PGDH knockout mice also showed significant protection from colitis-induced colon shortening (Fig. S15). Finally, SW033291-treated mice displayed a significant reduction in the levels of colitis-associated inflammatory cytokines, including TNF, IL-1 beta, interferon gamma, IL-2, CCL2, and CCL4 (Fig. S16).

To identify the cellular mediators responsible for the protective effect of 15-PGDH inhibition, we constructed chimeric mice from 15-PGDH wild-type mice that received bone marrow transplants from either 15-PGDH wild-type or 15-PGDH knockout marrow donors. The two groups of chimeric mice showed identical susceptibility to DSS-induced colitis as measured by disease activity, weight loss, and total percentage of ulcerated mucosa (Figs. S17, S18). These results suggest that colitis protection is due to inhibition of 15-PGDH in colonocytes, which are the primary site of 15-PGDH expression in the colon (33), rather than to inhibition of 15-PGDH in bone marrow -derived cells.

To further characterize the mechanism by which 15-PGDH inhibition protects the colon epithelium, we assessed the effects of SW033291 on cell proliferation in the colon crypts. On day 8, after 7 days of oral DSS treatment, wild-type mice receiving concurrent injections with vehicle-control showed significant suppression of BrdU incorporation in colonic crypts (Figs. 5, S19). In contrast, day 8 BrdU incorporation was increased 2.5-fold in SW033291-treated animals (Fig. 5B, 10 mg/kg SW033291) and increased 2.4-fold in 15-PGDH knockout mice (Fig. 5C). Immunofluorescence staining for cleaved caspase 3 showed only

scattered apoptotic cells, and these were present in similar amounts in control and SW033291-treated mice. Thus 15-PGDH inhibition appears to confer protection primarily by helping maintain colonocyte proliferation in the DSS -damaged mucosa.

15-PGDH Inhibition Promotes Liver Regeneration

We next examined the effects of 15-PGDH inhibition on regeneration in the liver. Inhibiting 15-PGDH increases PGE2 levels in this organ (Fig. 1, A and B); and provocatively, COX-2 inhibitors antagonize regrowth of the liver after surgery (11, 34, 35). We found that after resection of two-thirds of the liver mass (35), both 15-PGDH knockout mice and SW033291-treated wild-type mice showed a markedly increased rate and extent of liver regeneration as compared to wild-type mice treated with vehicle-control (Figs. 6A–C). Although the 15-PGDH knockout and wild-type mice had equal pre-operative liver weights, the knockout mice attained 28% and 40% greater total liver weight than controls on post-operative days (POD) 3 and 4, respectively (Fig. 6, A and B). Liver regeneration was similarly greater in SW033291-treated mice, which attained higher liver weights than controls on each of post-operative days 2 through 7 (Fig. 6C). Between post-operative days one through 7, SW033291-treated mice regenerated 77% greater new liver weight (0.48 gram increase) than did controls (0.27 gram increase) (Fig. 6C). Hepatocytes in SW033291-treated mice displayed a burst of proliferation on post-operative day 2: 40% of hepatocytes showed labeling with BrdU in treated mice versus 16% in vehicle-control treated mice (Fig. 6, D–F).

Consistent with SW033291 up-regulating prostaglandin signaling, regenerating livers of SW033291-treated mice showed 36–55% higher levels of cyclic AMP from post-operative days1 through 3 ($P<0.002$, Student’s t-test) (Fig. S20). However, we did not find differences between livers of SW033291-treated versus control mice in other downstream signaling targets, including levels of beta-catenin protein; nuclear localization of beta-catenin; and levels of phosphorylation at PKA target sites on CREB serine 133, beta-catenin serine 675, and beta-catenin serine 552 (10, 11).

Discussion

In summary, we have shown that 15-PGDH negatively regulates tissue regeneration and repair in the bone marrow, the colon, and the liver. While bone marrow, colon, and liver each demonstrate very different tissue architectures, in each of these tissues this biological function of 15-PGDH is conserved, suggesting a biological generality of this pathway. PGE2 and dmPGE2 show activities that favor tissue regeneration when used to treat cells in culture and when administered to animals in pharmacological doses (11, 13–16, 18, 24–27). Our findings further imply that in normal in vivo physiology, prostaglandins play a widespread homeostatic role in the maintenance and repair of injury across multiple body tissues. Indeed, our results show that a doubling of tissue PGE2 levels is able to markedly potentiate tissue repair. Of most direct utility, our observations identify 15-PGDH as a therapeutic target and provide a chemical formulation, SW033291, that is an active 15-PGDH inhibitor in vivo and that potentiates repair in multiple tissues.

15-PGDH inhibitors, such as SW033291, may have applicability to human HSC transplantation by potentially increasing transplant safety and reducing the required time of hospitalization (1). The mechanism of SW033291, which activates the bone marrow niche of transplant recipients, is distinct from the effect of treating donor hematopoietic stem cells ex vivo with dmPGE2. Ex vivo treatment with dmPGE2 instead activates the donor stem cells, for example by up-regulating donor cell expression of CXCR4 (the CXCL12 receptor) (15, 16). These prior and current studies together thus identify, respectively, two independent PGE2 responsive pathways for potentiating HSC transplants, one targeted by the ex vivo dmPGE2 treatment of donor hematopoietic stem cells, and the other by in vivo SW033291 administration to HSC transplant recipients. The use of granulocyte colony-stimulating factor to assist neutrophil recovery after HSC transplant provides one precedent for the therapeutic utility of tissue regeneration approaches (36, 37). Distinguishing features of SW033291 are that in addition to accelerating neutrophil recovery (by a different approach), this 15-PGDH inhibitor accelerates regeneration of platelets and red blood cells, and also expands the numbers of more primitive bone marrow SKL cells. We anticipate 15-PGDH inhibitors would potentiate bone marrow regeneration after HSC transplants that employ either autologous or allogeneic derived stem cells, which are most often harvested from the donor's peripheral blood (1). As SW033291 also enables successful murine bone marrow reconstitution from a reduced inoculum of marrow cells, SW033291 may additionally have applicability to HSC transplants that employ human umbilical cord blood stem cells, in which numbers of donor cells are limited by supply and expense (2, 3).

15-PGDH inhibitors, such as SW033291, may also have applicability to treatment of human ulcerative colitis. Mucosal healing is increasingly recognized as a significant therapeutic goal in treatment of this disease (5, 38). The activity of SW033291 in stimulating colon epithelial regeneration in the mouse DSS colitis model suggests potential applicability to this treatment need. 15-PGDH inhibitors, such as SW033291, may also have therapeutic applicability to humans undergoing surgical resection of primary liver tumors or of colon cancers metastatic to the liver. In both these cases, patient's eligibility for surgery is limited by the requirement that the post-operative liver remnant be sufficient to enable regenerating an adequate liver mass (6–8).

Previous studies from our group have shown that 15-PGDH shows tumor suppressor activity in colon cancer, but yet that many individuals have low 15-PGDH expression levels in their colonic mucosa (22, 39–41). These current observations suggest one explanation for this seeming paradox may be that in certain biological contexts, such as in bowel injury, low levels of colonic 15-PGDH may provide a biological advantage by potentiating faster organ recovery. More generally, this study provides an example in which the regulated and short-term inhibition of a tumor suppressor gene may provide therapeutic utility without adverse effect, particularly in a disease contextin which tissue repair is the immediate medical goal.

Supplementary Material

Refer to Web version on PubMed Central for supplementary material.

Acknowledgments

We thank the members of the UT Southwestern HTS Core facility for their support of the high throughput screen; A Dannenberg, D. Montrose, and M. Datt for helpful scientific discussions; and K. Lingas, B. Maitra, and J. Ren for helpful technical support. Funded by NIH grants P50 CA150964 (S.D.M.), P30 CA043703 (S.L.G.), R25CA148052 (Y.Z.), U54HL119810 (Paul DiCorleto), 1P01CA95471-09 (Steven McKnight, J.M.R.), 5P30 CA142543-03 (The Simmons Cancer Center, (J.K.V.W.)) which support the UT Southwestern HTS Core Facility, P50 CA130810 (Dean Brenner), P30 DK097948 (F.C.), and by Scholar Innovator Award from the Harrington Discovery Institute (S.D.M.), and by grants from the Marguerite Wilson Foundation (S.D.M.), Inje University (S.Y.Y. and K.B.B.), and NRF-MSIP of Korea 2014002213 (K.B.B), and the Welch Foundation (I-1612, J.M.R.), and CPRIT (RP110708), and by gifts from the Leonard and Joan Horvitz Foundation (S.D.M) and the Richard Horvitz and Erica Hartman-Horvitz Foundation (S.D.M.). Case Western Reserve University, the University of Texas, and the University of Kentucky have filed patent applications (PCT/US2013/036790; PCT/US2013/036790) related to SW033291 and other 15-PGDH inhibitors and their use in the treatment of disease.

References and Notes

1. Copelan EA. Hematopoietic stem-cell transplantation. N Engl J Med. 2006; 354:1813–1826. [PubMed: 16641398]
2. Norkin M, Lazarus HM, Wingard JR. Umbilical cord blood graft enhancement strategies: has the time come to move these into the clinic? Bone Marrow Transplant. 2013; 48:884–889. [PubMed: 22941377]
3. Fares I, et al. Cord blood expansion. Pyrimidoindole derivatives are agonists of human hematopoietic stem cell self-renewal. Science. 2014; 345:1509–1512. [PubMed: 25237102]
4. Cutler C, et al. Prostaglandin-modulated umbilical cord blood hematopoietic stem cell transplantation. Blood. 2013; 122:3074–3081. [PubMed: 23996087]
5. Danese S, Fiocchi C. Ulcerative colitis. N Engl J Med. 2011; 365:1713–1725. [PubMed: 22047562]
6. Benson AB 3rd, et al. NCCN clinical practice guidelines in oncology: hepatobiliary cancers. J Natl Compr Canc Netw. 2009; 7:350–391. [PubMed: 19406039]
7. Tsai MS, et al. Clinicopathological features and prognosis in resectable synchronous and metachronous colorectal liver metastasis. Annals of surgical oncology. 2007; 14:786–794. [PubMed: 17103254]
8. Hayashi M, et al. Clinicopathological analysis of recurrence patterns and prognostic factors for survival after hepatectomy for colorectal liver metastasis. BMC Surg. 2010; 10:27. [PubMed: 20875094]
9. Brown JR, DuBois RN. COX-2: a molecular target for colorectal cancer prevention. J Clin Oncol. 2005; 23:2840–2855. [PubMed: 15837998]
10. Castellone MD, Teramoto H, Williams BO, Druey KM, Gutkind JS. Prostaglandin E2 promotes colon cancer cell growth through a Gs-axin-beta-catenin signaling axis. Science. 2005; 310:1504–1510. [PubMed: 16293724]
11. Goessling W, et al. Genetic interaction of PGE2 and Wnt signaling regulates developmental specification of stem cells and regeneration. Cell. 2009; 136:1136–1147. [PubMed: 19303855]
12. Barker N, et al. Identification of stem cells in small intestine and colon by marker gene Lgr5. Nature. 2007; 449:1003–1007. [PubMed: 17934449]
13. Frisch BJ, et al. In vivo prostaglandin E2 treatment alters the bone marrow microenvironment and preferentially expands short-term hematopoietic stem cells. Blood. 2009; 114:4054–4063. [PubMed: 19726721]
14. North TE, et al. Prostaglandin E2 regulates vertebrate haematopoietic stem cell homeostasis. Nature. 2007; 447:1007–1011. [PubMed: 17581586]
15. Hoggatt J, Singh P, Sampath J, Pelus LM. Prostaglandin E2 enhances hematopoietic stem cell homing, survival, and proliferation. Blood. 2009; 113:5444–5455. [PubMed: 19324903]
16. Goessling W, et al. Prostaglandin E2 enhances human cord blood stem cell xenotransplants and shows long-term safety in preclinical nonhuman primate transplant models. Cell stem cell. 2011; 8:445–458. [PubMed: 21474107]

17. Hoggatt J, Mohammad KS, Singh P, Pelus LM. Prostaglandin E2 enhances long-term repopulation but does not permanently alter inherent stem cell competitiveness. Blood. 2013; 122:2997–3000. [PubMed: 24047650]
18. Jung P, et al. Isolation and in vitro expansion of human colonic stem cells. Nat Med. 2011; 17:1225–1227. [PubMed: 21892181]
19. Kabashima K, et al. The prostaglandin receptor EP4 suppresses colitis, mucosal damage and CD4 cell activation in the gut. The Journal of clinical investigation. 2002; 109:883–893. [PubMed: 11927615]
20. Tai HH, Ensor CM, Tong M, Zhou H, Yan F. Prostaglandin catabolizing enzymes. Prostaglandins Other Lipid Mediat. 2002; 68–69:483–493.
21. Coggins KG, et al. Metabolism of PGE2 by prostaglandin dehydrogenase is essential for remodeling the ductus arteriosus. Nat Med. 2002; 8:91–92. [PubMed: 11821873]
22. Myung SJ, et al. 15-Hydroxyprostaglandin dehydrogenase is an in vivo suppressor of colon tumorigenesis. Proc Natl Acad Sci U S A. 2006; 103:12098–12102. [PubMed: 16880406]
23. Copeland, RA. Enzymes. A Practical Introduction to Structure, Mechanism, and Data Analysis. Wiley-VCH; New York: 2000. p. 305-317.
24. Hagedorn EJ, Durand EM, Fast EM, Zon LI. Getting more for your marrow: boosting hematopoietic stem cell numbers with PGE2. Experimental cell research. 2014; 329:220–226. [PubMed: 25094063]
25. Pelus LM, Hoggatt J, Singh P. Pulse exposure of haematopoietic grafts to prostaglandin E2 in vitro facilitates engraftment and recovery. Cell proliferation. 2011; 44(Suppl 1):22–29. [PubMed: 21481039]
26. Porter RL, et al. Prostaglandin E2 increases hematopoietic stem cell survival and accelerates hematopoietic recovery after radiation injury. Stem Cells. 2013; 31:372–383. [PubMed: 23169593]
27. Hoffman CM, Calvi LM. Minireview: complexity of hematopoietic stem cell regulation in the bone marrow microenvironment. Mol Endocrinol. 2014; 28:1592–1601. [PubMed: 25083740]
28. Morrison SJ, Scadden DT. The bone marrow niche for haematopoietic stem cells. Nature. 2014; 505:327–334. [PubMed: 24429631]
29. Pelus LM, Broxmeyer HE, Kurland JI, Moore MA. Regulation of macrophage and granulocyte proliferation. Specificities of prostaglandin E and lactoferrin. The Journal of experimental medicine. 1979; 150:277–292. [PubMed: 313430]
30. Okayasu I, et al. A novel method in the induction of reliable experimental acute and chronic ulcerative colitis in mice. Gastroenterology. 1990; 98:694–702. [PubMed: 1688816]
31. Becker C, et al. In vivo imaging of colitis and colon cancer development in mice using high resolution chromoendoscopy. Gut. 2005; 54:950–954. [PubMed: 15951540]
32. Cooper HS, Murthy SN, Shah RS, Sedergran DJ. Clinicopathologic study of dextran sulfate sodium experimental murine colitis. Laboratory investigation; a journal of technical methods and pathology. 1993; 69:238–249.
33. Yan M, et al. 15-Hydroxyprostaglandin Dehydrogenase, a COX-2 oncogene antagonist, is a TGF-β induced suppressor of human gastrointestinal cancers. Proc Natl Acad Sci U S A. 2004; 101:17468–17473. [PubMed: 15574495]
34. Rudnick DA, Perlmutter DH, Muglia LJ. Prostaglandins are required for CREB activation and cellular proliferation during liver regeneration. Proc Natl Acad Sci U S A. 2001; 98:8885–8890. [PubMed: 11447268]
35. Mitchell C, Willenbring H. A reproducible and well-tolerated method for 2/3 partial hepatectomy in mice. Nature protocols. 2008; 3:1167–1170.
36. Bendall LJ, Bradstock KF. G-CSF: From granulopoietic stimulant to bone marrow stem cell mobilizing agent. Cytokine Growth Factor Rev. 2014; 25:355–367. [PubMed: 25131807]
37. Metcalf D. Hematopoietic cytokines. Blood. 2008; 111:485–491. [PubMed: 18182579]
38. Lichtenstein GR, Rutgeerts P. Importance of mucosal healing in ulcerative colitis. Inflamm Bowel Dis. 2010; 16:338–346. [PubMed: 19637362]

39. Yan M, et al. 15-Hydroxyprostaglandin dehydrogenase inactivation as a mechanism of resistance to celecoxib chemoprevention of colon tumors. Proc Natl Acad Sci U S A. 2009; 106:9409–9413. [PubMed: 19470469]

40. Fink SP, et al. Aspirin and the risk of colorectal cancer in relation to the expression of 15-hydroxyprostaglandin dehydrogenase (HPGD). Science translational medicine. 2014; 6:233re232.

41. Thompson CL, et al. Genetic variation in 15-hydroxyprostaglandin dehydrogenase and colon cancer susceptibility. PLoS One. 2013; 8:e64122. [PubMed: 23717544]

42. Tong M, Tai HH. Synergistic induction of the nicotinamide adenine dinucleotide-linked 15-hydroxyprostaglandin dehydrogenase by an androgen and interleukin-6 or forskolin in human prostate cancer cells. Endocrinology. 2004; 145:2141–2147. [PubMed: 14749354]

43. Niesen FH, et al. High-affinity inhibitors of human NAD-dependent 15-hydroxyprostaglandin dehydrogenase: mechanisms of inhibition and structure-activity relationships. PLoS One. 2010; 5:e13719. [PubMed: 21072165]

44. Zhang X, et al. Epitope tagging of endogenous proteins for genome-wide ChIP-chip studies. Nat Methods. 2008; 5:163–165. [PubMed: 18176569]

45. Zhang JH, Chung TD, Oldenburg KR. A Simple Statistical Parameter for Use in Evaluation and Validation of High Throughput Screening Assays. Journal of biomolecular screening. 1999; 4:67–73. [PubMed: 10838414]

46. Wu Z, Liu D, Sui Y. Quantitative assessment of hit detection and confirmation in single and duplicate high-throughput screenings. Journal of biomolecular screening. 2008; 13:159–167. [PubMed: 18216390]

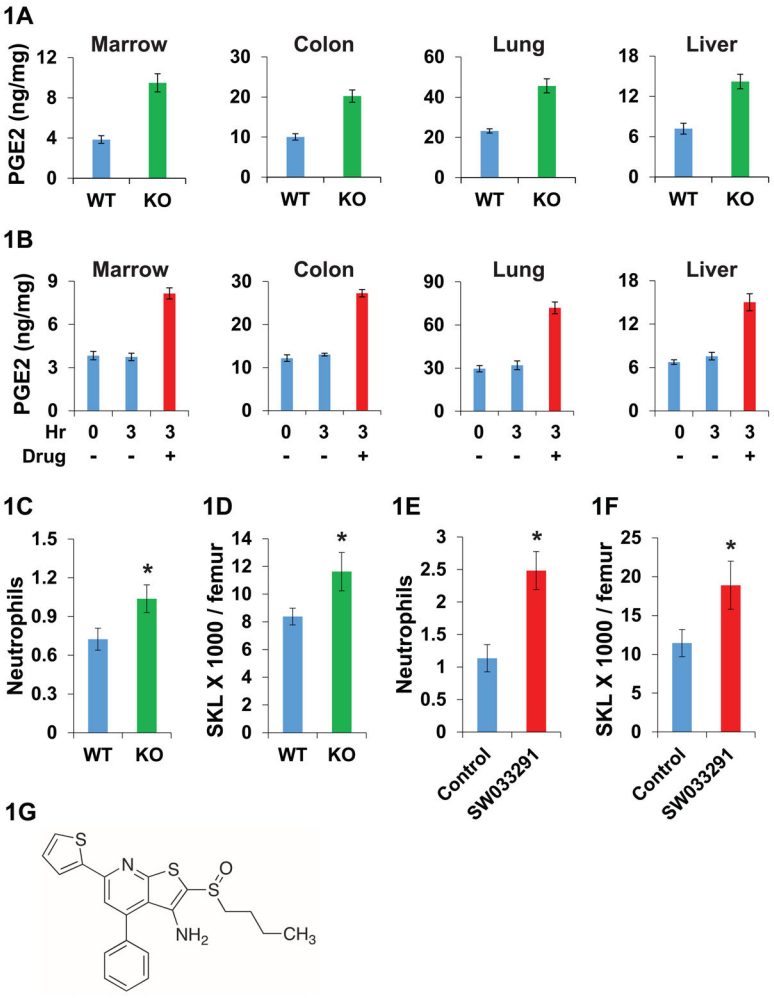

Fig. 1. Biological effects of 15-PGDH inhibition in mice

(A) PGE2 levels (ng PGE2/mg protein) in 15-PGDH knockout (KO) and wild-type (WT) mouse tissues. N=5 mice per data point. (B) PGE2 levels in tissues of mice at 0 hour baseline and at 3 hours after IP injections with either 10 mg/kg SW033291 (drug), or with vehicle-control. N=6 mice per data point. (C) Neutrophil counts from FVB 15-PGDH WT versus KO mice. Y-axis scale: 10^3 cells/μl. * indicates P=0.031, Student's t-test. N=16 mice per data point. (D) SKL cell numbers in bone marrow of FVB 15-PGDH WT versus KO mice. Y-axis scale: 10^3 cells/femur. * indicates P<0.04, Student's t-test. N=16 mice per data point. (E, F) Comparison of C57BL/6J mice treated with SW033291 (10 mg/kg IP twice daily for 5 doses) versus vehicle-control. (E) Neutrophil counts. Y-axis scale: 10^3 cells/μl. * indicates P<0.003, Student's t-test. N=6 SW033291 treated and 9 control mice. (F) SKL cell numbers in bone marrow. Y-axis scale: 10^3 cells/femur. * indicates P=0.039, Student's t-test. N=9 SW033291 treated and 12 control mice. (G) Chemical structure of SW033291. All graphs show means +/− standard error of the means (SEM).

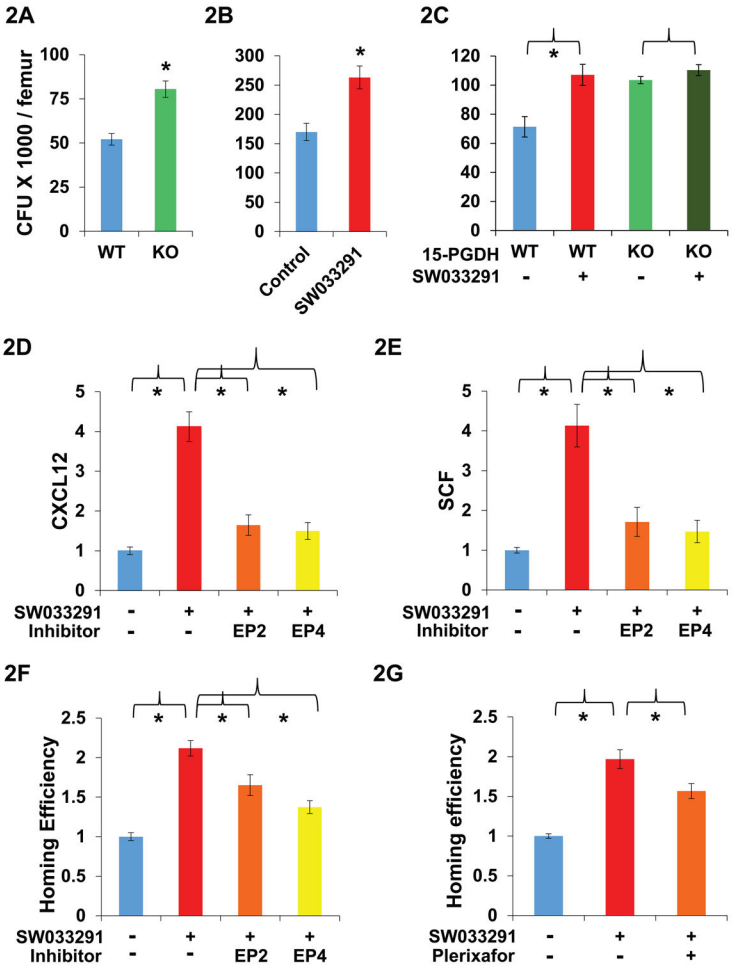

Fig. 2. Effect of 15-PGDH inhibition on bone marrow

(A–C) Y-axis graphs comparison of hematopoietic colony forming units generated per femur on day 14 after plating mouse bone marrow cells into methylcellulose with cytokines. (A) Bone marrow from FVB 15-PGDH wild-type (WT) versus knockout (KO) mice. N=4 mice plated in duplicate per data point. * indicates P<0.003, Student's t-test. (B) Bone marrow from SW033291-treated (10 mg/kg IP twice daily for 5 doses) versus vehicle-control-treated C57BL/6J mice. N=4 mice plated in duplicate per data point. * indicates P<0.009, Student's t-test. (C) Bone marrow from FVB WT or KO mice treated ex vivo with SW033291 (+) versus vehicle-control (−). N=3 mice plated in duplicate per data point. * indicates P<0.025, Student's t-test. (D, E) Gene induction in $CD45^{-}$ bone marrow cells from mice treated with SW033291 (+) or with vehicle-control (−) in combination with: the EP2 antagonist PF-04418948 (EP2), the EP4 antagonist L-161,982 (EP4), or control diluent (−). N=4 pools of 3 mice each per data point. * indicates P<0.02 compared to mice treated with SW033291 but without an EP receptor antagonist, Student's t-test. (D) Relative CXCL12 expression. (E) Relative SCF expression. (F, G) Homing of CFSE labeled donor marrow cells to the bone marrow of irradiated mice, comparing SW033291-treated versus vehicle-control-treated recipient mice. Y-axis graphs homing efficiency determined as the ratio at 16 hours of % CFSE labeled cells in the marrows of (SW033291-treated mice)/(vehicle-treated

mice). N=9 mice per data point. Graphs show comparison of recipient mice treated with SW033291 (+) or with vehicle-control (−) in combination with control diluent (−) or with the antagonists indicated. (F) EP2 antagonist PF-04418948 (EP2) or EP4 antagonist L-161,982 (EP4). * indicates $P<0.013$ versus mice receiving only SW033291, Student's t-test. (G) CXCL12 antagonist Plerixafor. * indicates $P<0.019$ versus mice receiving only SW033291, Student's t-test. All graphs show means +/− SEM.

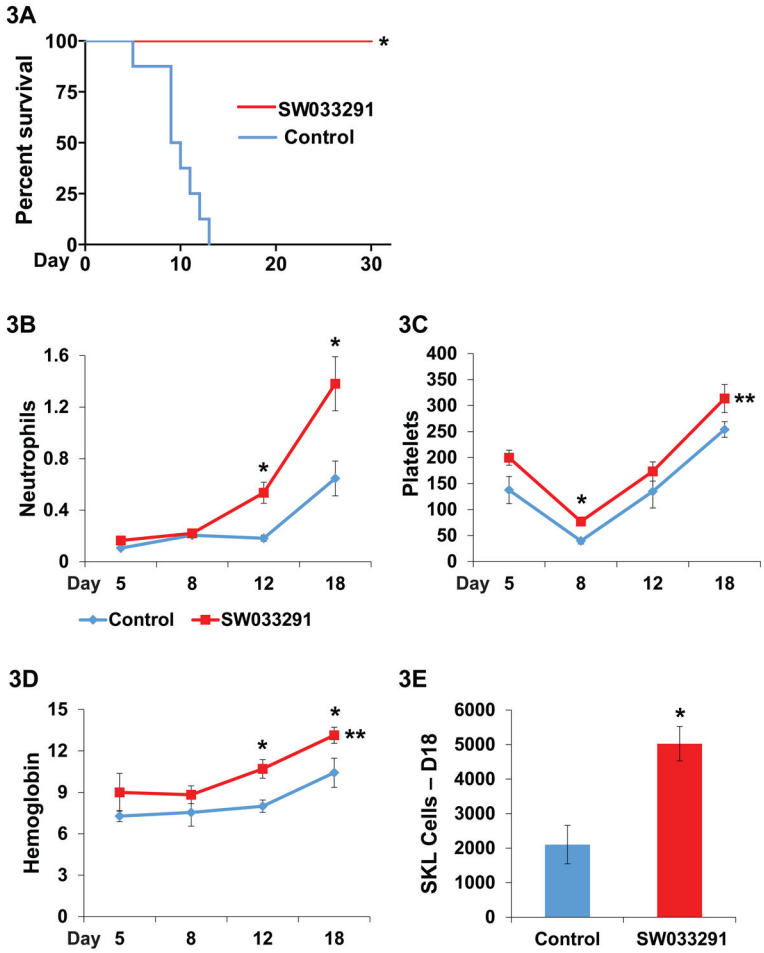

Fig. 3. SW033291 potentiates hematopoietic recovery after bone marrow transplantation

(A) Survival of mice lethally irradiated with 11 Gy following transplantation with 200,000 bone marrow cells plus treatment with IP injection ofSW033291, 5mg/kg twice daily, or with vehicle-control. N=8 mice in each cohort. * indicates P<0.0001 for increased survival in SW033291-treated mice, Log-rank test. (B–E) Recovery of peripheral blood counts in mice lethally irradiated with 11 Gy followed by transplantation with 500,000 bone marrow cells. Transplanted mice received treatments with twice daily IP injection of SW033291 5mg/kg (SW033291) or vehicle-control (Control). Parallel transplanted cohorts were assayed on post-transplant day 5 (group 1, N=4 control and 4 treated mice), day 8 (group 2, N=4 control and 4 treated mice), and days 12 and 18 (group 3, N=8 control and 10 treated mice, plus two deceased control mice). (B) Neutrophil counts. Y-axis scale: 10^3 cells/μl. * indicates P<0.014 on days 12 and 18, Student's t-test. On days 5 and 8, total white blood cell counts are substituted for neutrophil counts, as values were too low for meaningful differential counts. (C) Platelet counts. Y-axis scale: 10^3 cells/μl. * indicates P<0.003 on day 8, Student's t-test. ** indicates P=0.005 for comparison of platelet recovery across days 5–18, paired Student's t-test. (D) Hemoglobin level. Y-axis scale: g/dL. * indicates P≤0.03 on days 12 and 18, Student's t-test. ** indicates P<0.01 for comparison of hemoglobin recovery across days 5–18, paired Student's t-test. (E) Number of SKL bone marrow cells per mouse

on day 18 post-transplant. Data are means from N=8 control and 10 treated mice. * indicates P<0.0013, Student's t-test. All graphs show means +/− SEM.

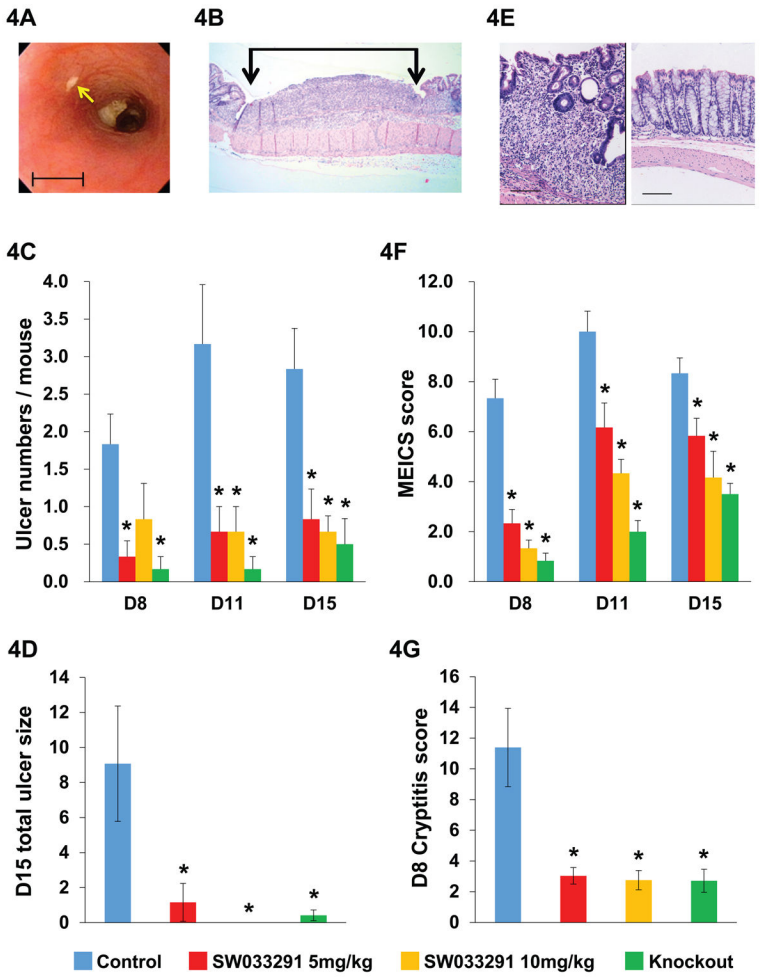

Fig. 4. 15-PGDH inhibition protects mice from DSS-induced colitis

(A) Colonoscopic view of a DSS-induced colon ulcer (arrow). Scale bar=1 mm. (B) Microscopic image of a DSS induced colon ulcer (between vertical arrows) Scale bar=2.3 mm. (C, D, F, G) Effects of administering 7 days of DSS compared between experimental groups of: vehicle-control-treated mice (blue), SW033291-treated mice (5mg/kg IP twice daily) (red), SW033291-treated mice (10mg/kg IP twice daily) (gold), and 15-PGDH knockout mice (green). (C) Graph of mean number of colon ulcers per DSS treated mouse counted by colonoscopy on study days 8, 11 and 15 (D8, D11, D15) for: vehicle-control-treated mice, SW033291-treated mice (5 mg/kg IP twice daily), SW033291-treated mice (10 mg/kg IP twice daily), and 15-PGDH knockout mice. N=6 mice for each data point. Anova $P<10^{-6}$. * indicates P<0.016 in daily subgroup comparisons to vehicle-control-treated mice, Student's t-test. (D) Graph depicts percentage of total colon length covered by ulcers on study day 15, determined by histomorphometric assessment (as in (B)) for DSS treated mice in cohorts of: vehicle-control-treated mice (N=7), SW033291-treated mice (5 mg/kg IP twice daily) (N=8), SW033291-treated mice (10 mg/kg IP twice daily) (N=8), and 15-PGDH knockout mice (N=9). Anova P<0.003. * indicates P<0.05 versus vehicle-control-treated mice, Student's t-test. (E) Left panel: representative photomicrograph of grade 2 cryptitis and mucosal thickening (on a 0–4 scale). Right panel: normal colon. Scale bars=100 μm. (F)

Graph of mean murine endoscopic index of colitis severity score (MEICS) in same mice as in (C). Anova $P<10^{-6}$. * indicates $P<0.024$ in daily comparisons to vehicle-control-treated mice, Student's t-test. (G) Graph of mean total colon cryptitis score (0–16 scale) on study day 8 for DSS treated mice in cohorts of: vehicle-control-treated mice (N=7), SW033291-treated mice (5 mg/kg IP twice daily) (N=8), SW033291-treated mice (10 mg/kg IP twice daily) (N=8), and 15-PGDH knockout mice (N=6). Anova $P<0.0005$. * indicates $P<0.022$ versus vehicle-control-treated mice, Student's t-test. All graphs show means +/− SEM.

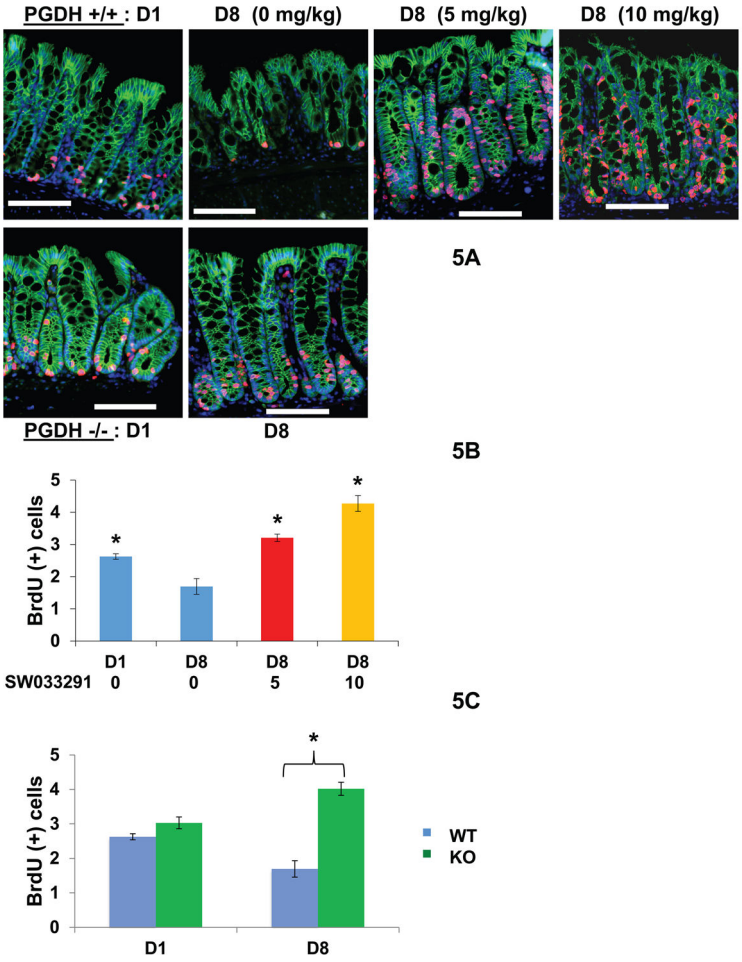

Fig. 5. 15-PGDH inhibition increases BrdU incorporation in colonic crypts

BrdU incorporation assessed in crypts of DSS treated mice. (A) Immunofluorescence visualization of BrdU incorporation (red), E-Cadherin stained crypts (green), and DAPI stained nuclei (blue) from distal colon. Upper panel shows photomicrographs of 15-PGDH wild-type mice (15-PGDH +/+) at pre-DSS baseline day 1 (D1) and then at day 8 (D8), following 7 days administration of DSS concurrent with twice daily IP injections with either 0, 5 mg/kg, or 10 mg/kg SW033291. Lower panel shows photomicrographs of 15-PGDH knockout (15-PGDH −/−) mice at pre-DSS baseline day 1 (D1), and at day 8 (D8) upon completion of DSS. Scale bars=50 μm. (B) Graphical plots of average number of BrdU positive cells per crypt in mice from upper panel of (A). N=6 mice for day 1, and N=8 mice for each day 8 data point. Anova P<0.0001. * indicates P<0.013 versus day 8 mice injected with 0 mg/kg SW033291 (i.e., vehicle-control), Student's t-test. (C) Graphical plots of average number of BrdU positive cells per crypt in day 1 (D1) baseline and day 8 (D8) DSS-treated mice that are 15-PGDH wild-type (WT) versus 15-PGDH knockout (KO). N= 6 to 8 mice per group. Anova P<0.0001. * indicates P< 3×10^{-5}, Student's t-test. All graphs show means +/− SEM.

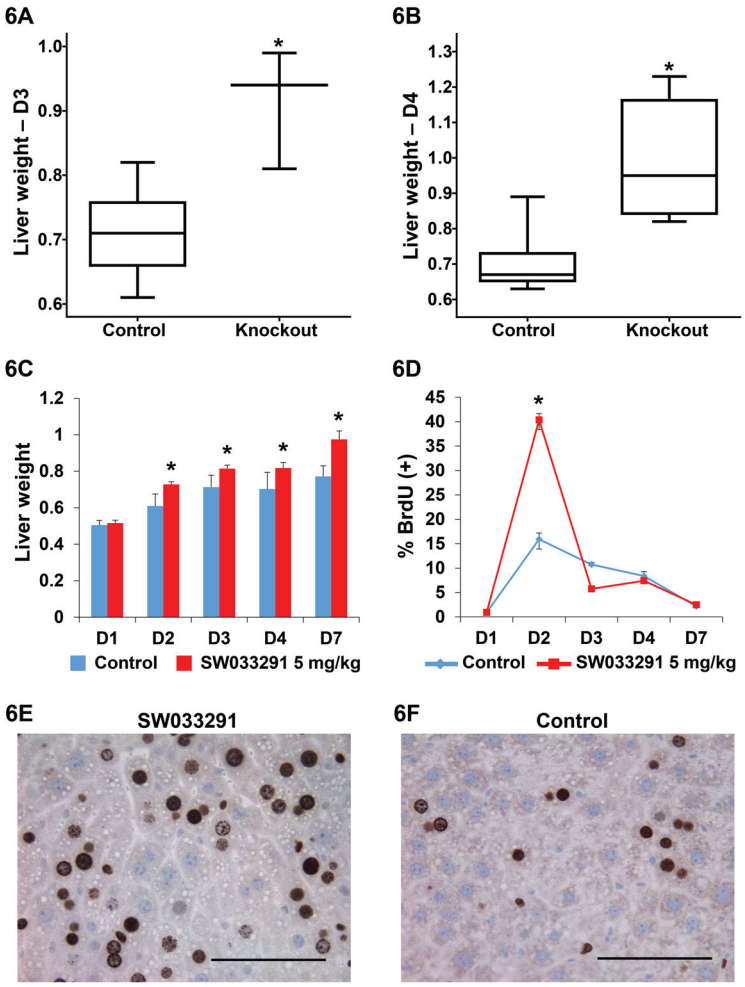

Fig. 6. Liver regeneration in mice after partial hepatectomy

(A, B) Box plots of regenerated liver weight (grams) attained after partial hepatectomy in control and 15-PGDH knockout mice. (A) Post-operative Day 3 (D3). N=10 control mice and N=3 knockout mice. * indicates P<0.0014, Student's t-test. (B) Post-operative-Day 4 (D4) N=10 control mice and N=6 knockout mice. * indicates P<0.0005, Student's t-test. (C) Total liver weight (grams) attained after partial hepatectomy (Y-axis) in mice injected IP twice daily with vehicle-control or SW033291 at 5 mg/kg across post-operative days 1–7 (D1–D7). Each value is mean of N=10 mice. * indicates P<0.011, Student's t-test. (D–F) BrdU incorporation following partial hepatectomy. (D) % BrdU positive cells (Y-axis) in vehicle-control-treated versus SW033291-treated mice on post-operative days 1–7 (D1–D7) (X-axis). Each value is the mean of from 6 to 10 mice. Error bars are smaller than symbols at nearly all data points. * indicates $P<1.0\times10^{-17}$ for postoperative day 2 comparison of SW033291-treated and control mice, Student's t-test. (E, F) Representative high-powered micrograph fields of BrdU staining hepatocytes on post-operative day 2 in SW033291-treated mice (E) and vehicle-control-treated mice (F). Scale bar=100 μm. All graphs show means +/− SEM.